RSC Advances

ROYAL SOCIETY OF CHEMISTRY

www.rsc.org/advances

A Conceptual DFT Study of the Hydrogen Trapping Efficiency in Metal Functionalized BN System

Madhu Samolia and T. J. Dhilip Kumar*

Department of Chemistry

Indian Institute of Technology Ropar

Rupnagar 140001, India

(Dated: June 5, 2014)

Abstract

The hydrogen trapping efficiency of metal functionalized BN system at various high electron density sites is studied using the first-principles conceptual density functional theory employing the M05-2X/6-311G+(d) level of theory. Metals are functionalized at three regions of BN system, namely borazine, having high nucleus independent chemical shift values. H_2 is trapped on the metal sites resulting in $B_3N_3H_XM_iH_m$ clusters [M = Li, Sc, Ti, V; X = 3,6; i = 1-3; m up to 30]. Global reactivity attributes have been computed which obey maximum hardness and minimum electrophilicity principles. Adsorption energy for physisorbed hydrogen is found to be low with Kubas-Niu interaction. Sc and Ti functionalized systems exhibit combination of hydrogen chemisorption and physisorption phenomenon with storage capacity in the range of 11.0 to 13.2 hydrogen wt %. These simple metal functionalized systems can be building block for assembling into two dimensional sheet or multidecker complex making it a potential hydrogen storage material.

Keywords: Adsorption, Conceptual DFT, Hydrogen storage, Nucleus independent chemical shift, Electrophilicity

*Electronic address: dhilip@iitrpr.ac.in

1. INTRODUCTION

Due to depleting resources and ever increasing demand, fossil fuels not only lead to the near future energy crisis but also ravage the earth's atmosphere by emission of CO_2 resulting in global warming. Hydrogen energy is considered to be a best alternative for future demand because of its renewable, highest energy density per unit mass and environmental friendly nature since produces water when used in fuel cell.[1, 2] However, transition to hydrogen economy depends on three major issues, viz., the hydrogen generation, its storage in a safe and economic mode, and efficient distribution for use. Hydrogen being light weight gas storage in tanks in the compressed form requires sufficiently large volume and tank made of expensive composite material, and in the cryogenic liquid form requires very low temperature. The best alternative of storing hydrogen is in solid materials. The ideal solid storage system should be stable, have high hydrogen reversibility and low adsorption energy.[3, 4]

Until now, many materials have been explored to make an efficient hydrogen storage system for transport applications. During the last two decades, a large number of templates like hydrides,[5–7] metal organic frameworks,[8–14] graphenes,[15, 16] covalent organic frameworks[17–19] and zeolites,[20, 21] alanates,[22, 23] clathrates,[24] metal clusters,[25–27] etc. have been investigated. Although considerable work has been carried out to design new hydrogen storage materials, currently, no material is meeting the US Department of Energy (DOE) target[28] of hydrogen gravimetric density of 9.0% and volumetric capacity of 81 g L^{-1} by 2015 for usable specific energy from H_2. As each material is having its own pros and cons searching for new and better alternatives for hydrogen storage is an important area of contemporary research. In general, the bonding of hydrogen is either too strong, or too weak and hence rather difficult to attain all desired storage parameters, simultaneously. The target parameters for hydrogen storage materials can only be attained if the hydrogen binding energy is retained in between that of the physisorption and chemisorption energies.[29]

The promising materials of hydrogen storage are the systems that possess boron and nitrogen atoms since they can be constructed into BN structural motif. Such motif produces π electron cloud on the top and bottom of the plane similar to benzene. Hence metal

atoms can be doped and hydrogen can be loaded on to the metal sites which will result in chemisorption or physisorption or combination of both. This is due to charge transfer between metal and π electron cloud resulting in reduced availability of charge at the metal site for binding with H_2 with binding energies intermediate between physisorption and chemisorption, which will make the system hydrogen reversible. The metal atoms interact with the BN π electron cloud by Dewar coordination[30] and simultaneously binds to H_2 by Kubas interaction.[31, 32] Earlier, it has been found that metal decorated organic complexes such as C_6H_6, $B_3N_3H_6$ etc. exhibit promising hydrogen storage properties[33–35] as they can be constructed into two dimensional graphene, BN sheets or three dimensional carbon, BN nanotubes, respectively. Experiments performed on the pristine BN nanotubes showed that it could only uptake 2.6 wt % hydrogen while Pt metal functionalized nanotube enhanced storage capacity to 4.2 wt % under 10 MPa pressure at room temperature.[36, 37]

Theoretical calculations of hydrogen adsorption on metal functionalized borazine and BN nanotube systems have been studied by various groups. Shevlin *et al.* have performed the GGA-PW91 calculations and found that various transition metals bind to top of borazine with Sc and Ti having higher binding energy while Cr and Mn have lower binding energy.[38] Largely, the binding of transition metal in BN system is milder than in benzene. Unfortunately, the GGA-PW91 functional used in their study is insufficient to describe dispersion interactions. Li *et al.* have studied the hydrogen storage in borazine decorated with Li, Na, K and Ti metals from the sides only at the B end without the substituted H atom.[39] The decoration on the borazine ring π cloud have not been considered. Hydrogen storage capacity of Ti, Ni, Rh, and Pd functionalized on single-walled BN nanotubes have been studied by Durgun and Zhang groups.[40, 41] Wu *et al.* have studied the H_2 adsorption properties of Pt metal dimer doped on BN nanotubes.[42] The adsorption of H_2 on Ce-doped BN nanotubes have been investigated and concluded that 5.7 hydrogen wt % can be stored in the system.[43]

In this paper, the density functional theory (DFT) calculations performed using reliable hybrid functionals for hydrogen storage on light metal atoms such as Li, Sc, Ti and V functionalized on to $B_3N_3H_6$ ring from different sides is reported. The objective of the present study is to identify the structural and electronic properties of hydrogen adsorption on

stable $B_3N_3H_XM_i$ system by computing nucleus independent chemical shift (NICS) values,[44] interaction energy, hydrogen adsorption energy and global reactivity descriptors. This study will be useful in designing metal functionalized BN system to develop novel nanostructures capable of trapping hydrogen with high storage densities and favorable energetic properties. This work is the complementary study of Weck *et al.* which is limited to hydrogen storage in C_mH_mM (M = Sc, Ti, V; m = 4-6) systems[45] and also to bridge, and extend the earlier theoretical studies on BN systems. The paper is organized as follows: The details of the computational methodology are given in section 2, followed by presentation of results and discussion in section 3. A summary of our findings and conclusions are given in section 4.

2. COMPUTATIONAL DETAILS

The molecular geometries of $B_3N_3H_XM_i$ (X = 3, 6; i = 1−3; M = Li, Sc, Ti, V) and their corresponding H_2 trapped analogues are optimized using the DFT's M05-2X functional[46] employing 6-311+G(d) basis sets as implemented in the Gaussian-09 program.[47] The metal atoms functionalized are at their ground state configurations. M05-2X is a functional with double the amount of non-local exchange and hence effective in representing weak non-bonded intermolecular and dispersion interactions. It is reported to be effective in incorporating electron spin density, density gradient, kinetic energy density, and Hartree-Fock (HF) exchange.[48–53] Harmonic vibrational analysis is performed to confirm the stability of the system which resulted in all positive frequencies.

The stability of metal functionalized BN system is studied by computing binding energy using the expression,

$$E_b = \frac{1}{i}[E_{B_3N_3H_XM_i} - (iE_M + E_{B_3N_3H_X})] \quad (1)$$

where $E_{B_3N_3H_XM_i}$ is the total energy of M_i-BN system, $E_{B_3N_3H_X}$ is the energy of $B_3N_3H_X$ and E_M is the energy of M atom while i stands for number of M atoms.

The adsorption energy per hydrogen, E_{ad}, of metal-BN system is calculated by

$$E_{ad} = \frac{1}{n}[E_{B_3N_3H_XM_i} + nE_{H_2} - E_{B_3N_3H_XM_iH_m}] \quad (2)$$

where $E_{B_3N_3H_XM_iH_m}$ is the total energy of number of hydrogen molecules (n) adsorbed on M_i-BN system where $m = 2n$ and E_{H_2} is the energy of isolated H_2 molecule.

The stability of hydrogen saturated metal functionalized BN system is studied by computing interaction energy, ΔE, which is negative of adsorption energy, E_{ad}, reported in kcal mol^{-1}. Global reactivity descriptors such as electronegativity,[54] hardness,[55] and electrophilicity[56] are used as tools for analyzing the stability and reactivity of the studied systems using the conceptual DFT.[57] Such descriptors are calculated as defined below.

For a system having N-electrons with total energy E, the electronegativity (χ) and hardness (η) are obtained as follows

$$\chi = -\left(\frac{\partial E}{\partial N}\right)_{\nu(r)} \tag{3}$$

and

$$\eta = \left(\frac{\partial^2 E}{\partial N^2}\right)_{\nu(r)} \tag{4}$$

where $\nu(r)$ represents external potential.

If vertical ionization potential (I) and vertical electron affinity (A) are calculated using Koopman's theorem,[58] then, η is expressed as

$$\eta = I - A \tag{5}$$

and χ is expressed as

$$\chi = \frac{I + A}{2} \tag{6}$$

Electrophilicity, (ω), is defined as

$$\omega = \frac{\chi^2}{2\eta} \tag{7}$$

The kinetic stability of the metal functionalized BN system is studied by evaluating their energy separation between the highest occupied molecular orbitals (HOMOs) and lowest unoccupied molecular orbitals (LUMOs), E_g.

3. RESULTS AND DISCUSSION

Borazine is functionalized with various metals such as Li, Sc, Ti and V. Aromaticity of the borazine has been computed on the basis of NICS values. A negative value of NICS indicates aromatic while positive values indicate anti-aromatic and more negative the value, more aromatic the system. NICS values are calculated at three different positions (1) in center of borazine ring (2) 1 Å above and below the center of the ring and (3) sides of the ring away from B-N bonds. In the center, NICS value is found to be -0.84 ppm, while from 1 Å above and below the center of the ring has -2.26 ppm. In the sides of the ring, close to B-N bonds, NICS values have been found to be -3.25, -3.31, and -3.54 ppm. NICS value is very low in the center of the ring but has high value above and below the ring. This indicates presence of π electron density on the top and bottom of the ring, as in benzene.

Due to presence of high electron density, metals are functionalized in borazine from these three regions through Dewar coordination. When the H_2 is introduced sequencially on the M functionalied BN system, some metals results in H_2 chemisorption initially, while further introduction of H_2 results in physisorption. The H_2 and metal forms Kubas type bonding where the H_2 molecule donate electrons to the empty *d*-orbitals of the metal atom which back donate electrons to the anti-bonding orbital of the H_2 molecule leading to chemisorption. The physisorption is due to the charge polarization mechanism[59, 60] proposed by Niu *et al.* where the charge on the metal atom, created due to charge transfer from BN, polarizes the H_2 molecule resulting in the near molecular bonding of H_2. Such interaction is also known in the Ti doped C_5H_5, C_4H_4 and C_8H_8 systems.[61]

3.1. $B_3N_3H_6M$ (M = Li, Sc, Ti and V)

Metal atom (M) is bound to $B_3N_3H_6$ above the ring where M = Li, Sc, Ti and V and its binding energy E_b is computed. E_b is found to be positive indicating the metal propensity to bound on the π electron cloud of borazine. H_2 is introduced sequentially on the metal site and their geometries are optimized. Optimized geometries of $B_3N_3H_6MH_m$ where $m = 2n$ are shown in Figure 1. Metal doped borazine is found to accommodate maximum 2 H_2 molecules in Li, 4 in Sc and V, while 6 in Ti. The calculated interaction energy, ΔE,

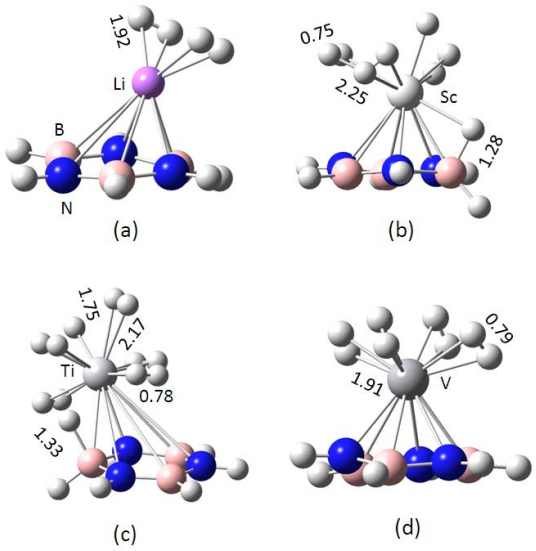

FIG. 1: Optimized structures of (a) $B_3N_3H_6LiH_4$, (b) $B_3N_3H_6ScH_8$, (c) $B_3N_3H_6TiH_{12}$ and (d) $B_3N_3H_6VH_8$.

for $B_3N_3H_6LiH_4$ is found to be -3.0 kcal mol^{-1}. For transition metals the ΔE is found to be -13.5, -10.1 and -11.5 kcal mol^{-1} for $B_3N_3H_6ScH_8$, $B_3N_3H_6TiH_{12}$, and $B_3N_3H_6VH_8$, respectively, as shown in Table I. The reactivity descriptors have been computed using the equations (5)-(7). As the number of H_2 molecules increases, the hardness (η) increases while the electrophilicity (ω) decreases which indicates the increase in the stability of the system according to maximum hardness principle[62] and minimum electrophilicity principle.[63] Upon adsorption of H_2 molecules, the hardness is found to be maximum for $B_3N_3H_6TiH_{12}$ reaching 7.10 eV while it is minimum for $B_3N_3H_6LiH_4$ of 4.27 eV. Electrophilicity marginally increased for $B_3N_3H_6TiH_{12}$ to 0.73 eV when compared to $B_3N_3H_6Ti$ system (0.36 eV) while maximum for $B_3N_3H_6VH_8$ of 4.35 eV. Electronegativity decreases up on adsorption of H_2 molecules in case of Li, and V and it increases in case of Sc, and Ti. The HOMO-LUMO energy gap, E_g, increases after adsorbing the H_2 molecules for all the systems which indicates the increase in the kinetic stability. It is maximum for Ti reaching 7.3 eV, and minimum for Li with 3.5 eV. $B_3N_3H_6MH_m$ system is found to have hydrogen wt % of 12.8% in case of Ti, 10.5% for Sc, 10.0% for V and 6.6 wt % for Li.

Adsorption energy, E_{ad}, has been calculated and plotted against the number of H_2

TABLE I: Calculated binding energy (E_b), interaction energy/H_2 ($\triangle$E), electronegativity (χ), hardness (η), electrophilicity (ω), and the HOMO-LUMO gap (E_g) of $B_3N_3H_6M$ and the H_2 trapped $B_3N_3H_6M$ systems. The corresponding hydrogen wt % is also given.

System	E_b (eV)	$\triangle$E (kcal mol^{-1})	χ (eV)	η (eV)	ω (eV)	E_g (eV)	H wt %
$B_3N_3H_6Li$	0.16		2.20	2.83	0.86	3.0	
$B_3N_3H_6LiH_4$		-3.0	2.08	4.27	0.51	3.5	6.6
$B_3N_3H_6Sc$	0.55		2.72	3.91	0.94	4.0	
$B_3N_3H_6ScH_8$		-13.5	3.08	6.00	0.79	6.0	10.5
$B_3N_3H_6Ti$	1.38		2.0	5.53	0.36	3.6	
$B_3N_3H_6TiH_{12}$		-10.1	3.22	7.10	0.73	7.3	12.8
$B_3N_3H_6V$	6.77		8.04	4.58	7.06	6.0	
$B_3N_3H_6VH_8$		-11.5	7.73	6.87	4.35	7.2	10.0

molecules in Figure 2. The quantum effect of zero point energy due to the hydrogen molecules reduces the magnitude of static adsorption energy up to 25 %.[64] Two H_2 molecules physisorbed on Li metal have low E_{ad} value of $\sim$0.2 eV. In Sc, the first hydrogen molecule results in chemisorption where H_2 molecule splits into H atoms. One H atom is attached to the Sc atom having Sc-H bond length 1.91 Å while other H atom bridge with B atom having B-H bond length 1.28 Å and Sc-H bond length 2.15 Å. Introduction of second hydrogen molecule onwards results in physisorption phenomenon. For Sc atom, maximum adsorption energy is found to be 1.9 eV for first chemisorbed hydrogen molecule and least for fourth adsorbed hydrogen molecule with the value of 0.6 eV. Adsorption energy is highest for the first hydrogen molecule as it is chemisorbed while decreases gradually as the introduced H_2 are physisorbed.

When Ti is doped on the borazine E_{ad} is found to be high as 1.5 eV for first chemisorbed H_2 molecule and decreases gradually for physisorbed H_2 molecules reaching to 0.4 eV. For accommodating all six hydrogen molecules on Ti, one chemisorbed hydrogen move to B atom. It is observed that B-H bond length is 1.33 Å and the H atom moved to form bridge

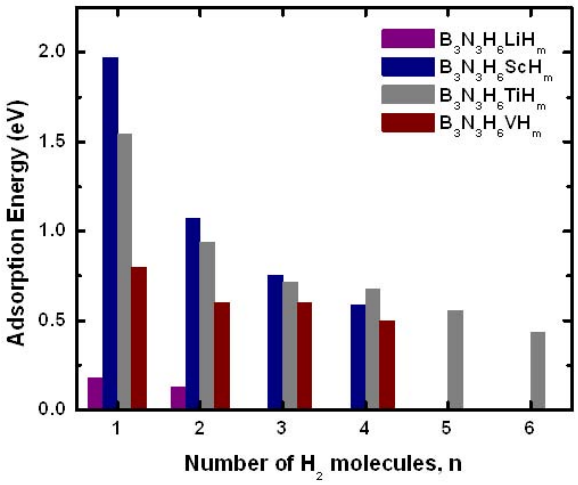

FIG. 2: Adsorption energy of $B_3N_3H_6MH_m$ system as a function of number of H_2 molecules, n, where $m = 2n$.

TABLE II: Average bond lengths of metal to chemisorbed H atom (M-H_c), metal to physisorbed H atom (M-H_p) and H-H of H_2 saturated $B_3N_3H_6M$ systems.

System	M-H_c (Å)	M-H_p (Å)	H-H (Å)
$B_3N_3H_6LiH_4$		1.91	0.76
$B_3N_3H_6ScH_8$	1.91	2.25	0.75
$B_3N_3H_6TiH_{12}$	1.75	1.98	0.78
$B_3N_3H_6VH_8$		1.91	0.77

between Ti and B having Ti-H bridge distance is 1.98 Å. Second chemisorbed H atom remains attached on Ti atom with Ti-H bond length of 1.75 Å. To accommodate all five hydrogen molecules on Ti, Ti is shifted to side of the ring as structure is slightly distorted. In the case of V, all 4 H_2 are physisorbed with adsorption energy for first adsorbed hydrogen molecule is found to be highest of 0.77 eV and decreases attaining 0.5 eV for the fourth physisorbed hydrogen molecule.

The changes in variation in the bond lengths with respect to metal and chemisorbed hydrogen (M-H_c), metal and physisorbed hydrogen (M-H_p) and H-H in the $B_3N_3H_6MH_m$

TABLE III: Calculated binding energy (E_b), interaction energy/H_2 ($\triangle$E), electronegativity (χ), hardness (η), electrophilicity (ω), and the HOMO-LUMO gap (E_g) of $B_3N_3H_XM_2$ and the H_2 trapped $B_3N_3H_XM_2$ systems. The corresponding hydrogen wt % is also given.

System	E_b (eV)	$\triangle$E (kcal mol^{-1})	χ (eV)	η (eV)	ω (eV)	E_g (eV)	H wt %
$B_3N_3H_3Li_2$	0.71		5.17	7.39	2.58	7.3	
$B_3N_3H_3Li_2H_{12}$		-1.7	4.97	7.15	1.72	7.6	14.5
$B_3N_3H_6Sc_2$	0.08		3.12	3.53	1.38	2.1	
$B_3N_3H_6Sc_2H_{16}$		-11.4	3.02	6.76	0.67	5.3	11.8
$B_3N_3H_6Ti_2$	0.94		2.70	0.94	3.90	3.6	
$B_3N_3H_6Ti_2H_{16}$		-13.9	2.97	6.80	0.65	6.5	11.5
$B_3N_3H_6V_2$	9.31		14.56	5.98	17.74	4.7	
$B_3N_3H_6V_2H_{16}$		-13.6	11.96	6.24	11.46	7.1	11.1

are provided in Table II. The average H-H distances have increased in all the systems as compared to isolated H_2 distance of 0.741 Å.

3.2. $B_3N_3H_XM_2$ (X = 3, 6; M = Li, Sc, Ti and V)

Two M atoms are functionalized on the top and bottom positions of $B_3N_3H_6$ where M = Li, Sc, Ti and V and their binding energy is found to be positive. H_2 is introduced sequentially on the metal functionalized sites. Optimized geometries of $B_3N_3H_XM_2H_m$ systems where m up to 16 are shown in Figure 3. The structure of $B_3N_3H_6Li_2$ is found to be distorted hence $B_3N_3H_3Li_2$ and $B_3N_3H_4Li_2$ structures are explored. The stability of the two systems is studied by computing the binding energy. For $B_3N_3H_3Li_2$, binding energy is 0.71 eV while for $B_3N_3H_4Li_2$, binding energy is found to be 0.28 eV. $B_3N_3H_3Li_2$ is chosen for H_2 adsorption study due to its high binding energy. $B_3N_3H_XM_2$ system with Li is found to accommodate maximum of 6 H_2 molecules 3 each on top and bottom sites, while Sc, Ti, and V sites can accommodate 8 H_2 molecules each with 4 each on top and bottom sites. The interaction energy of 6 H_2 molecules adsorbing to system containing Li resulting

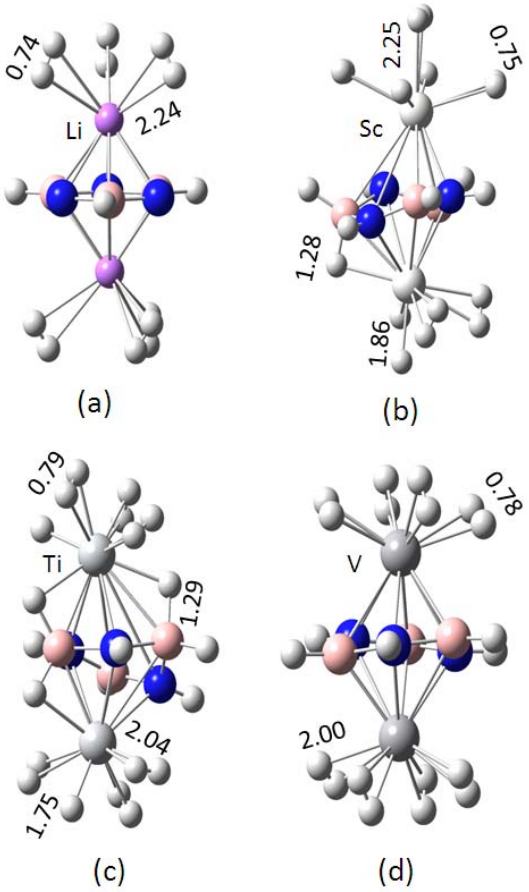

FIG. 3: Optimized structures of H_2 saturated (a) $B_3N_3H_3Li_2H_{12}$, (b) $B_3N_3H_6Sc_2H_{16}$, (c) $B_3N_3H_6Ti_2H_{16}$ and (d) $B_3N_3H_6V_2H_{16}$.

to $B_3N_3H_3Li_2H_{12}$ is found to be -1.7 kcal mol^{-1} while interaction energy of 8 H_2 molecules adsorbing to system containing Sc, Ti and V resulting to $B_3N_3H_6Sc_2H_{16}$, $B_3N_3H_6Ti_2H_{16}$ and $B_3N_3H_6V_2H_{16}$ are found to be -11.4, -13.9, and -13.6 kcal mol^{-1}, respectively. It is observed that the interaction energy is found to increase gradually as more H_2 is introduced on the metal atoms.

Hardness and electrophilicity follows the similar trend for $B_3N_3H_XM_2H_m$ as that of $B_3N_3H_6MH_m$ except system containing Li where it marginally decreases as shown in Table III. Hardness increases for systems containing Sc, Ti and V. In case of Ti, there is surge in hardness value from 0.94 eV to 6.80 eV as the number of adsorbed H_2 molecules increases. A reverse trend is observed in case of electrophilicity as compared to hardness which obeys

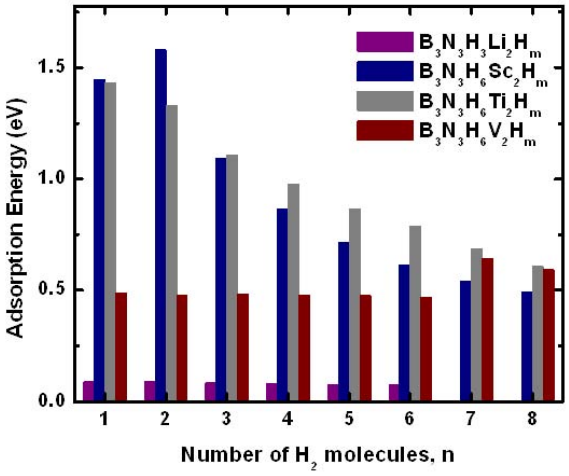

FIG. 4: Adsorption energy of $B_3N_3H_XM_2H_m$ system as a function of number of H_2 molecules, n, where $m = 2n$ and $X = 3$, 6.

maximum hardness and minimum electrophilicity principles. All the clusters exhibit decrease in electrophilicity upon adsorbing H_2 molecules. Electronegativity of $B_3N_3H_XM_2H_m$ decreases for Li, Sc, and V containing systems while it increases for Ti system. Hydrogen wt % is found to be 14.5% for Li, 11.8% for Sc, 11.5% for Ti and 11.1% for V. Although Li containing system has high hydrogen wt % its interaction energy is found to be very low with a value of -1.7 kcal mol^{-1} while other metal containing system is found to have high interaction energy ranging from -11.4 to -13.9 kcal mol^{-1}. The HOMO-LUMO energy gap increases for the $B_3N_3H_XM_2H_m$ system indicating increased kinetic stability. It is doubled after H_2 adsorption in Sc and Ti systems reaching 6.5 eV for Ti, and 5.3 eV for Sc containing systems.

Figure 4 shows the variation of adsorption energy with the sequential addition of H_2 molecules. Li has very low adsorption energy close to 0.1 eV where all 6 H_2 molecules are physisorbed with H-H distance slightly increased to 0.75 Å as shown in Figure 3(a). Adsorption energy is high for Sc containing system for the first and second chemisorbed H_2 molecules which is ∼1.5 eV. First H_2 molecule introduced on top Sc atom result in chemisorption phenomenon forming 2 Sc-H bonds with bond length of 1.84 Å. Second H_2 molecule introduced on bottom Sc atom also results in chemisorption with 1 H forming Sc-H bond with bond length 1.86 Å and other H forming Sc-H-B bridge bond in which Sc-H

TABLE IV: Average bond lengths of metal to chemisorbed H atom (M-H_c), metal to physisorbed H atom (M-H_p) and H-H of H_2 saturated $B_3N_3H_XM_2$ systems.

System	M-H_c (Å)	M-H_p (Å)	H-H (Å)
$B_3N_3H_3Li_2H_{12}$		2.28	0.74
$B_3N_3H_6Sc_2H_{16}$	1.84	2.25	0.76
$B_3N_3H_6Ti_2H_{16}$	1.75	2.00	0.78
$B_3N_3H_6V_2H_{16}$		1.96	0.77

bond length found to be 2.18 Å. Bond length of H-B bond is 1.28 Å as shown in Figure 3(b). Third H_2 onwards all the H_2 molecules get physisorbed with the adsorption energy decreasing gradually from 1.1 to 0.5 eV.

In case of $B_3N_3H_XM_2H_m$ system containing Ti the first and second H_2 molecules on each Ti is chemisorbed forming Ti-H bonds with bond lengths 1.75 and 1.73 Å. Third H_2 molecule exhibits physisorption phenomenon and to accommodate H_2, chemisorbed H atoms form Ti-H-B bridging bonds with bond length 1.94 Å for Ti-H, and 1.29 Å for H-B. Similar trend is also observed for the fourth H_2 molecule as the H_2 is introduced on second Ti from the bottom side of the $B_3N_3H_6$ ring as shown in Figure 3(c). As the first two H_2 molecules are chemisorbed the adsorption energy is found to be high with the value of 1.4 and 1.3 eV, respectively. From the third H_2 onwards result in physisorption with adsorption energy decreasing from 1.1 to 0.6 eV gradually as depicted in Figure 4. In V containing system, all the introduced H_2 molecules are physisorbed, similar to $B_3N_3H_6V$, as shown in Figure 3(d). Since all the H_2 molecules are physisorbed, the adsorption energy is found to be low falling in the range of 0.5-0.6 eV as shown in the Figure 4.

In Table IV the variation in the average bond length of chemisorbed and physisorbed M-H and H-H bonds are provided. The average H-H distances have increased in all the systems and the increase is longer in Ti and V systems and their Ti-H (2.00 Å), and V-H (1.96 Å) distances are shorter compared to Sc system indicating stronger interaction. This feature is also evident from their higher interaction and higher adsorption energies.

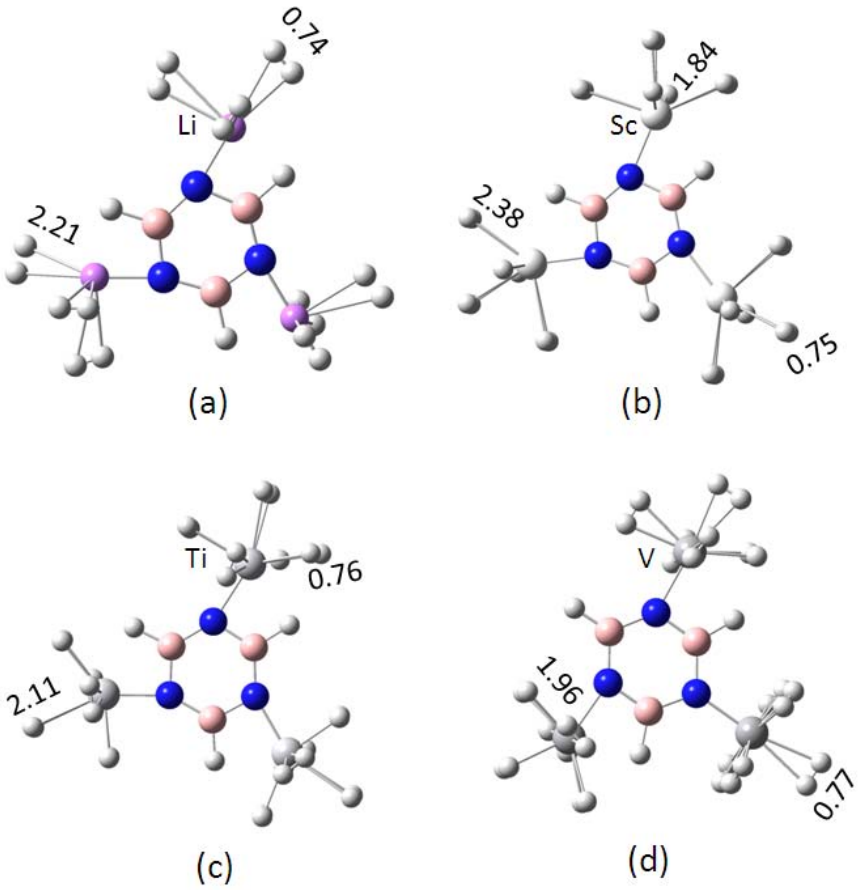

FIG. 5: Optimized structures of (a) $B_3N_3H_3Li_3H_{18}$, (b) $B_3N_3H_3Sc_3H_{24}$, (c) $B_3N_3H_3Ti_3H_{30}$ and (d) $B_3N_3H_3V_3H_{30}$.

3.3. $B_3N_3H_3M_3$ (M = Li, Sc, Ti and V)

Metals are functionalized on the equitorial sides of $B_3N_3H_6$ system away from B-N bonds as the electron density is found to be maximum. H atoms are also replaced to accommodate M which results in $B_3N_3H_3M_3$ system. M atoms bind to N ends of the borazine with positive binding energy. On the metal doped system, H_2 molecules are loaded resulting in maximum of three, four, five, and five H_2 on each Li, Sc, Ti and V functionalized systems, respectively, as shown in Figure 5(a)-(d). $B_3N_3H_3Li_3$ system can trap nine H_2 molecules resulting in the interaction energy of -1.5 kcal mol^{-1} while for Sc atoms results in -8.3 kcal mol^{-1} for 12 H_2 molecules. In Ti and V functionalized systems, interaction energy is found to be -9.5 and -7.2 kcal mol^{-1}, respectively, for 15 H_2 molecules. Interaction energy for Li

TABLE V: Calculated binding energy (E_b), interaction energy/H_2 ($\triangle$E), electronegativity (χ), hardness (η), electrophilicity (ω), and the HOMO-LUMO gap (E_g) of $B_3N_3H_XM_3$ and the H_2 trapped $B_3N_3H_XM_3$ systems. The corresponding hydrogen wt % is also given.

System	E_b (eV)	$\triangle$E (kcal mol^{-1})	χ (eV)	η (eV)	ω (eV)	E_g (eV)	H wt %
$B_3N_3H_3Li_3$	1.2		3.66	7.54	0.89	6.9	
$B_3N_3H_3Li_3H_{18}$		-1.5	3.46	7.47	0.80	7.0	18.1
$B_3N_3H_3Sc_3$	1.5		3.56	5.05	3.56	4.5	
$B_3N_3H_3Sc_3H_{24}$		-8.3	4.78	8.59	4.78	7.4	11.4
$B_3N_3H_3Ti_3$	1.9		14.7	3.3	32.5	6.3	
$B_3N_3H_3Ti_3H_{30}$		-9.5	13.7	6.7	14.1	6.8	13.2
$B_3N_3H_3V_3$	8.8		13.9	21.7	4.5	6.6	
$B_3N_3H_3V_3H_{30}$		-7.2	13.5	13.4	6.8	7.0	12.8

containing system is found to be lowest among all the systems.

Hardness for hydrogen adsorption increases from 5.0 eV to 8.5 for Sc and 3.3 to 6.7 eV for Ti while it remains same at 7.5 eV for Li functionalized $B_3N_3H_3M_3$ systems. Electrophilicity decreases from 0.89 to 0.80 eV for 9 H_2 adsorbed on Li system, 32.5 to 14.1 eV for 15 H_2 on Ti system, while increases from 3.6 eV to 4.8 eV for 12 H_2 on Sc system and 4.5 to 6.8 eV for 12 H_2 on V system due to H_2 adsorption. E_g also increases after adsorption of H_2 for all the $B_3N_3H_3M_3$ systems. For $B_3N_3H_3Li_3H_{18}$, hydrogen wt. % is found to be 18.1 which is interestingly very high but the system has very low interaction energy of -1.5 kcal mol^{-1} while it is 11.42 wt. % for $B_3N_3H_3Sc_3H_{24}$, 13.2 wt. % for $B_3N_3H_3Ti_3H_{30}$ and 12.8 wt. % for $B_3N_3H_3V_3H_{24}$ systems with high interaction energies ranging from -7.2 to -9.5 kcal mol^{-1}. The details of data obtained are provided in Table V.

Adsorption energy has been calculated for M functionalized BN regions and is shown in the Figure 6. Li system has very low adsorption energy (< 0.1 eV) since all the H_2 are physisorbed. Adsorption energy for Sc system is high ($\sim$1.0 eV) for the first three adsorbed

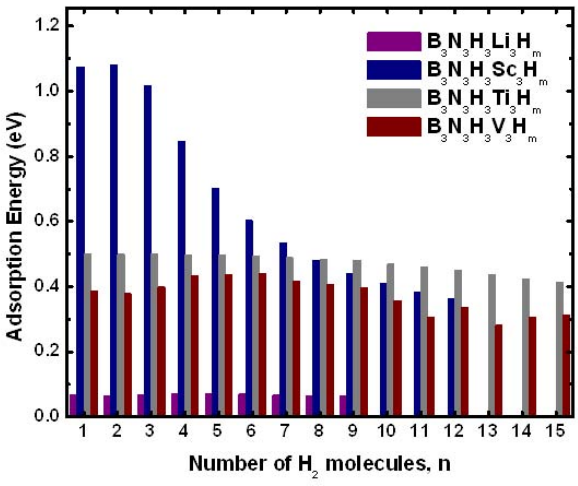

FIG. 6: Adsorption energy of $B_3N_3H_3M_3H_m$ system as a function of number of H_2 molecules, n, where $m = 2n$.

TABLE VI: Average bond lengths of metal to chemisorbed H atom (M-H_c), metal to physisorbed H atom (M-H_p) and H-H of H_2 saturated $B_3N_3H_3M_3$ systems.

System	M-H_c (Å)	M-H_p (Å)	H-H (Å)
$B_3N_3H_6Li_3H_{18}$		2.23	0.74
$B_3N_3H_6Sc_3H_{24}$	1.84	2.33	0.75
$B_3N_3H_6Ti_3H_{30}$		2.07	0.79
$B_3N_3H_6V_3H_{30}$		2.04	0.79

H_2 molecules as it leads to chemisorption in each metal. Then it decreases gradually to 0.35 eV when the Sc metal functionalized system is saturated with 12 H_2 molecules due to physisorption phenomenon. In Ti and V doped systems, 15 H_2 molecules physisorb resulting in low adsorption energy in the range of ∼0.5 and ∼0.4 eV, respectively. The average bond lengths of the M-H and H-H in case of $B_3N_3H_3M_3H_m$ systems are provided in Table VI. In Ti and V systems, the H-H bond lengths elongation is larger in magnitude (0.79 Å) than Li and Sc (∼0.75 Å) systems.

TABLE VII: Hirshfeld charges for metals on $B_3N_3H_3M_3$ and $B_3N_3H_3M_3H_6$ systems where M = Li, Sc, Ti, V and M_a, M_b, M_c are index numbers of M_3 atoms.

System	Hirshfeld charges	System	Hirshfeld charges
$B_3N_3H_3M_3$	M_a, M_b, M_c	$B_3N_3H_3M_3H_6$	M_a, M_b, M_c
	a.u.		a.u.
$B_3N_3H_3Li_3$	0.438, 0.440, 0.442	$B_3N_3H_3Li_3H_6$	0.340, 0.338, 0.342
$B_3N_3H_3Sc_3$	0.300, 0.270, 0.254	$B_3N_3H_3Sc_3H_6$	0.641, 0.640, 0.641
$B_3N_3H_3Ti_3$	1.072, 1.113, 1.071	$B_3N_3H_3Ti_3H_6$	0.961, 0.908, 0.900
$B_3N_3H_3V_3$	1.057, 1.007, 1.007	$B_3N_3H_3V_3H_6$	0.834, 0.895, 0.828

3.4. Hirshfeld charge analysis of $B_3N_3H_3M_3$

The first H_2 molecule functionalized on Sc_3 system result in chemisorption while Ti_3 and V_3 system results in physisorption. In order to account for the observed behavior the Hirshfeld charge analysis has been performed on the $B_3N_3H_3M_3$ system. Hirshfeld charges for metals before loading and after loading of 3 H_2 are tabulated in the Table VII. Transition metals having relatively large Hirshfeld charge (electron deficient) results in H_2 physisorption while with relatively low Hirshfeld charge (electron rich) result in chemisorption. Hirshfeld charge of Sc atoms is found to be ∼0.3 a.u. while Ti and V is ∼1.0 a.u. Due to relatively high electronic charge density, Sc bind strongly with the H_2 resulting in H-H bond breaking while Ti, and V have low electronic charge density resulting in weak binding with the H_2. The charge analysis of H_2 loaded Ti and V systems indicate that charge of the metal decreases to ∼0.9 and ∼0.8 a.u., respectively, indicating charge transfer taking place from H_2 to Ti, and V while, charge of the metal increases in Sc to ∼0.65 a.u. In Li system, considering that it is alkali metal, the Hirshfeld charge is found to be ∼0.4 a.u. which is weak to break H_2 bond and hence results in physisorption.

3.5. Electrostatic potential maps of $B_3N_3H_XM_i$

In order to understand the physisorption and chemisorption phenomenon exhibited by different metal functionalized BN systems, electrostatic potential maps superimposed

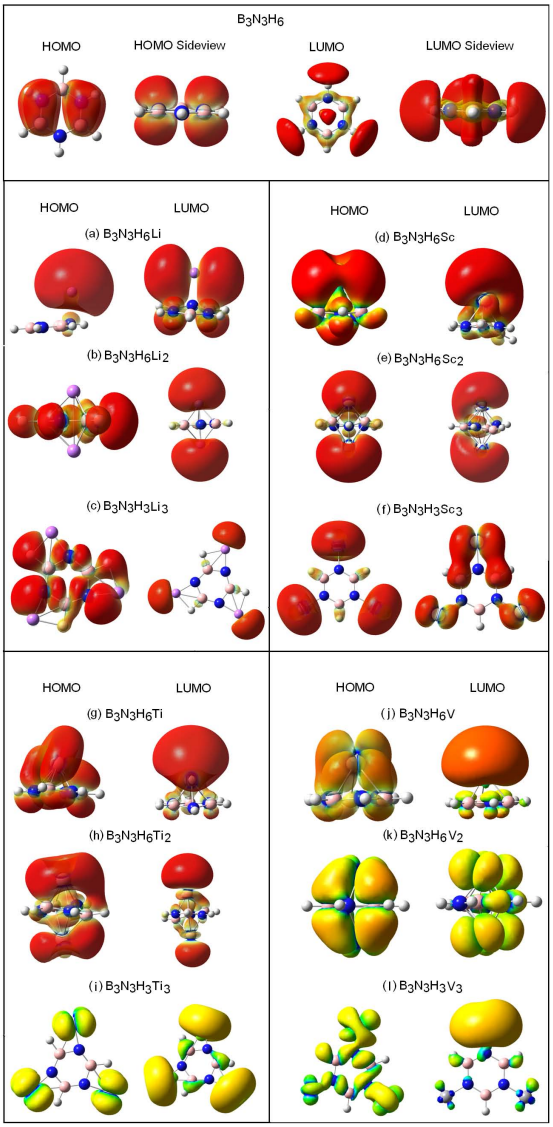

FIG. 7: Electrostatic potential maps superimposed on the HOMO and LUMO orbitals of $B_3N_3H_6$, $B_3N_3H_XLi_i$, $B_3N_3H_XSc_i$, $B_3N_3H_XTi_i$ and $B_3N_3H_XV_i$ clusters with i = 1-3 and X = 3, 6.

on the HOMO and LUMO orbitals of metal atoms binding to all the three regions of borazine resulting in $B_3N_3H_XM_i$ structures (M = Li, Sc, Ti, V; $i = 1{-}3$) are obtained and shown in Figure 7. The HOMO-LUMO energy gap, E_g, increases after adsorbing the H_2 molecules which indicates the increase in the kinetic stability of the system as shown in the Tables I, III, and V. The red color in the electron density plots indicates electron rich sites while green color indicates electron deficient sites. Also, isolated borazine molecule electrostatic potential maps superimposed on the HOMO and LUMO orbitals are shown.

On the sides of borazine, metal binds to N atom since it has electron rich orbital as shown in the figure. As evident from the plots in Figure 7 that H_2 chemisorption takes place in the $B_3N_3H_6Sc$ (d), $B_3N_3H_6Sc_2$ (e), $B_3N_3H_3Sc_3$ (f), $B_3N_3H_3Ti$ (g) and $B_3N_3H_6Ti_2$ (h) systems. The reduced electron density in the $B_3N_3H_3Ti_3$ (i) and all the V containing BN systems, $B_3N_3H_XV_i$ (j)-(l), are shown in green and yellow colors. Due to electron deficiency in such systems result in H_2 physisorption which is also confirmed from the high positive values of Hirshfeld charges for $B_3N_3H_3M_3$ [M = Ti, V] as provided in Table VII.

Simultaneous metal functionalization on all three electron rich sites of BN system, namely, on top, on bottom and on the side of B-N bonds at once resulting in $B_3N_3H_XM_i$ with i = 5 leads to clustering of metals similar to clustering of Ti on a C_{60} surface and reduction in the hydrogen storage capacity[65] and hence H_2 adsorption studies could not be performed on such systems.

4. SUMMARY AND CONCLUSIONS

In this paper, the hydrogen storage capacity of $B_3N_3H_XM_i$ system where M = Li, Sc, Ti and V has been studied using the first-principles density functional calculations employing the M05-2X/6-311G+(d) level of theory. Metals are functionalized on the top, bottom, and side of the borazine ring having high NICS value. By Dewar coordination metals are functionalized on the π electron cloud in borazine. Simultaneous metal functionalization on all three electron rich sites of BN system at once resulted in clustering of metals. H_2 is trapped on the metal sites resulting in $B_3N_3H_XM_iH_m$ clusters with m up to 30. H_2 loading in Li and V results in physisorption while in Sc and Ti initially there is chemisorption and with additional loading of H_2 results in physisorption. The adsorption energy for chemisorbed hydrogen is high while low for physisorbed hydrogen due to charge polarization mechanism.

The computed global reactivity attributes for the hydrogen adsorbed $B_3N_3H_XM_i$ system obeys maximum hardness and minimum electrophilicity principles indicating the high stability of the studied systems. The results indicate that Ti containing systems $B_3N_3H_3Ti_2H_{16}$ and $B_3N_3H_3Ti_3H_{30}$ can be used as high capacity storage media with 11.5 and 13.2 hydro-

gen wt %, respectively. This is closely followed by Sc containing systems, $B_3N_3H_6ScH_8$, $B_3N_3H_3Sc_2H_{16}$ and $B_3N_3H_3Sc_3H_{24}$ with the capacity of ∼11.0 wt %. Though $B_3N_3H_3Li_3H_{18}$ system has highest hydrogen storage capacity of ∼18 wt %, it could not be considered as storage material due to its low interaction energy resulting in less stability whereas transition metal-borazine system interaction energy is found to be high. These simple metal functionalized borazine systems can be used as building blocks for assembling into two dimensional sheet or multidecker complex making it a potential hydrogen storage material although their ability to reversibly trap H_2 is expected to decrese marginally.

Acknowledgements

This work is financially supported by the Department of Science and Technology, New Delhi (DST grant SR/FT/CS-85/2010) and the authors thank the IIT Ropar for providing computational resources.

Electronic Supplementary Information (ESI) Available

The internal coordinates of optimized geometries of $B_3N_3H_XM_i$ (X = 3, 6; i = 1−3; M = Li, Sc, Ti, V), their corresponding H_2 trapped analogues $B_3N_3H_XM_iH_m$ (m up to 30) and results of vibrational analysis of the stable structures are provided as supplementary information. The hydrogen dissociation mechanism pathway over Ti metal atom and adsorption process is also provided.

[1] L. Schlapbach and A. Zuttel, *Nature* 2001 **414**, 353-358.

[2] R. Coontz and B. Hanson, *Science* 2004, **305**, 957.

[3] J. Graetz, *Chem. Soc. Rev.* 2009, **38**, 73-82.

[4] P. Jena, *J. Phys. Chem. Lett.* 2011, **2**, 206-211.

[5] J. J. Reilly, *CRC Press: Cleveland, OH*, 1977, **2**, 13.

[6] F. Schuth, *Nature* 2005, **434**, 712-713.

[7] S.-I. Orimo, Y. Nakamori, J. R. Eliseo, A. Zuttel and C. M. Jensen, *Chem. Rev.* 2007, **107**, 4111-4132.

[8] N. L. Rosi, J. Eckert, M. Eddaoudi, D. T. Vodak, J. Kim, M. Okeeffe and O. M. Yaghi, *Science* 2003, **300**, 1127-1129.

[9] J. L. C. Rowsel and O. M. Yaghi, *Angew. Chem., Int. Ed.* 2005, **44**, 4670-4679.

[10] J. L. C. Rowsel and O. M. Yaghi, *J. Am. Chem. Soc.* 2006, **128**, 1304-1315.

[11] S. S. Han, J. L. Mendoza-Cortes and W. A. Goddard III, *Chem. Soc. Rev.,*. 2009, **38**, 1460-1476.

[12] S. S. Han, W.-Q. Deng and W. A. Goddard III, *Angew. Chem., Int. Ed.* 2007, **46**, 6289-6292.

[13] J. L. C. Rowsell, A. R. Millward, K. S. Park and O. M. Yaghi,*J. Am. Chem. Soc.* 2004, **126**, 5666-5667.

[14] A. Kuc, T. Heine, G. Seifert and H. A. Duarte, *Chem. Eur. J.* 2008, **14**, 6597-6660.

[15] K. Sillar, A. Hofmann and J. Sauer, *J. Am. Chem. Soc.* 2009, **131**, 4143-4150.

[16] I. Cabria, M. J. Lopez and J. A. Alonso, *J. Am. Phys. Soc.* 2008, **78**, 075415;

[17] G. H. V. Bertrand, V. K. Michaelis, T.-C. Ong, R. G. Griffin and M. Dinca, *Proc. Natl. Acad. Sci. USA.* 2013, **110**, 4923-4928.

[18] M. A. Millar, C.-Y. Wang and G. N. Merrill, *J. Phys. Chem. C.* 2009, **113**, 3222-3231.

[19] S. S. Han, H. Furukawa, O. M. Yaghi and W. A. Goddard III, *J. Am. Chem. Soc.* 2008, **130**, 11580-11581.

[20] H. Wu, W. Zhou and T. Yildirim, *J. Am. Chem. Soc.* 2007, **129**, 5314-5315.

[21] R. B. Rankin, J. Liu, A. D. Kulkarni and J. K. Johnson, *J. Phys. Chem. C.* 2009, **113**, 16906-16914.

[22] C. P. Balde, B. P. C. Hereijgers, J. H. Bitter and K. P. De Jong, *Angew. Chem., Int. Ed.*

2006, **45**, 3501-3503.

[23] I. Ljubic and D. C. Clary, *Phys. Chem. Chem. Phys.* 2010, **12**, 4012-4023.

[24] H. Lee,J.-W. Lee, D. Y. Kim, J. Park, Y.-T. Seo, H. Zeng,I. L. Moudrakovski, C. I. Ratcliffe and J. A. Ripmeester, *Nature*, 2005, **434**, 743-746.

[25] W.-Q. Deng, X. Xu and W. A. Goddard, *Phys. Rev. Lett.* 2004, **92**, 166103-166107.

[26] Q. Sun, P. Jena, Q. Wang and M. Marquez, *J. Am. Chem. Soc.* 2006, **128**, 9741-9745.

[27] T. J. D. Kumar, P. F. Weck and N. Balakrishnan, *J. Phys. Chem. C.* 2007, **111**, 7494-7500.

[28] FreedomCAR/DOE hydrogen storage technical targets, http://www1.eere.energy.gov/hydrogenandfuelcells/pdfs/freedomcar_targets_explanations.pdf, accessed on 10/04/2014.

[29] R. C. Lochan and M. Head-Gordon, *Phys. Chem. Chem. Phys.* 2006, **8**, 1357-1370.

[30] D. Michael and P. Mingos, *J. Organomet. Chem.* 2001, **635**, 1-8.

[31] G. J. Kubas, R. R. Ryan, B. I. Swanson, P. J. Vergamini and H. J. Wasserman, *J. Am. Chem. Soc.* 1984, **106**, 451-452.

[32] G. J. Kubas, *Metal Dihydrogen and σ-bond Complexes: Structure, Theory, and Reactivity, Kluwer Academic/Plenum, New York*, 2001.

[33] B. Huang, H. Lee, W. Duan and J. Ihm, *Appl. Phys. Lett.* 2008, **93**, 063107.

[34] E. Durgun, S. Ciraci, W. Zhou and T. Yildirim, *Phys. Rev. Lett.* 2006, **97**, 226102-226105.

[35] W. Zhou, T. Yildirim, E. Durgun and S. Ciraci, *Phys. Rev. B.* 2007, **76**, 085434-085442.

[36] R. Ma, Y. Bando, H. Zhu, T. Sato, C. Xu and D. Wu, *J. Am. Chem. Soc.*, 2002, **124**, 7672-7673.

[37] C. Tang, Y. Bando, X. Ding, S. Qi and D. Golberg, *J. Am. Chem. Soc.* 2002, **124**, 14550-14551.

[38] S. A. Shevlin and Z. X. Guo, *Appl. Phys. lett.* 2006, **89**, 153104.

[39] M. Li, J. Li, Q. Sun and Y. Jia, *J. Appl. Phys.* 2010, **108**, 064326.

[40] E.Durgun, Y.-R. Jang and S. Ciraci, *Phys. Rev B.* 2007, **76**, 073413-073416.

[41] L. P. Zhang and P. Wu, M. B. Sullivan, *J. Phys. Chem. C* 2011, **115**, 4289-4296.

[42] X. Wu, J. L. Yang and X. C. Zeng, *J. Chem. Phys.* 2006, **125**, 044704.

[43] Z.-W. Zhang, W.-T. Zheng and Q. Jiang, *Int. J. Hydrogen Energy.* 2012, **37**, 5090-5099.

[44] P. V. R. Schleyer, C. Maerker, A. Dransfeld, H. Jiao and N. J. R. V. E. Hommes, *J. Am. Chem. Soc.* 1996, **118**, 6317-6318.

[45] P. F. Weck, T. J. D. Kumar, E. Kim and N. Balakrishnan, *J. Chem. Phys.* 2007, **118**, 094703.

[46] Y. Zhao, N. E. Schultz and D. G. Truhlar, *J. Chem. Theory Comput.* 2006, **2**, 364-382.

[47] Gaussian 09, Revision D.01, M. J. Frisch, G. W. Trucks, H. B. Schlegel, G. E. Scuseria, M. A. Robb, J. R. Cheeseman, G. Scalmani, V. Barone, B. Mennucci, G. A. Petersson, H. Nakatsuji, M. Caricato, X. Li, H. P. Hratchian, A. F. Izmaylov, J. Bloino, G. Zheng, J. L. Sonnenberg, M. Hada, M. Ehara, K. Toyota, R. Fukuda, J. Hasegawa, M. Ishida, T. Nakajima, Y. Honda, O. Kitao, H. Nakai, T. Vreven, J. A. Montgomery, Jr., J. E. Peralta, F. Ogliaro, M. Bearpark, J. J. Heyd, E. Brothers, K. N. Kudin, V. N. Staroverov, R. Kobayashi, J. Normand, K. Raghavachari, A. Rendell, J. C. Burant, S. S. Iyengar, J. Tomasi, M. Cossi, N. Rega, J. M. Millam, M. Klene, J. E. Knox, J. B. Cross, V. Bakken, C. Adamo, J. Jaramillo, R. Gomperts, R. E. Stratmann, O. Yazyev, A. J. Austin, R. Cammi, C. Pomelli, J. W. Ochterski, R. L. Martin, K. Morokuma, V. G. Zakrzewski, G. A. Voth, P. Salvador, J. J. Dannenberg, S. Dapprich, A. D. Daniels, . Farkas, J. B. Foresman, J. V. Ortiz, J. Cioslowski, and D. J. Fox, Revision B.01; Gaussian, Inc.: Wallingford CT, 2010.

[48] Y. Zhao and D. G. Truhlar, *Theor. Chem. Acc.* 2008, **120**, 215-241.

[49] S. N. Steinmann and C. Corminboeuf, *J. Chem. Theory Comput.* 2010, **6**, 1990-2001.

[50] S. J. Kolmann, B. Chan and M. J. T. Jordan, *Chem. Phys. Lett.* 2008, **467**, 126-130.

[51] R. Das, P. K. Chattaraj, *J. Phys. Chem. A*, 2012 *116* 3259-3266.

[52] S. Pan, G. Merino and P. K. Chattaraj, *Phys. Chem. Chem. Phys.* 2012, **14**, 10345-10350.

[53] K. Gopalsamy, M. Prakash, R. Mahesh Kumar and V. Subramanian, *Int. J. Hydrogen Energy* 2012, **37**, 9730-9741.

[54] K. D. Sen and C. K. Jorgenson, *Springer, Berlin*, 1987, **vol 66**.

[55] R. G. Parr and R. G. Pearson, *J. Am. Chem. Soc.* 1983, **105**, 7512-7516.

[56] R. G. Parr, L. V. Szentpaly and S. Liu, *J. Am. Chem. Soc.* 1999, **121**, 1922-1924.

[57] P. K. Chattaraj, *Taylor & Francis/CRC Press, Florida*, 2009.

[58] T. A. Koopmans, *Physica*, 1933, **1** 104-113.

[59] J. Niu, B. K. Rao and P. Jena, *Phys. Rev. Lett.* 1992, **68**, 2277-2280.

[60] J. Niu, B. K. Rao and P. Jena, *Phys. Rev. B.* 1995, **51**, 4475-4484.

[61] B. Kiran, A. K. Kandalam and P. Jena, *J. Chem. Phys.* 2006, **124**, 224703.

[62] R. G. Parr and P. K. Chattaraj, *J. Am. Chem. Soc.* 1991, **113**, 1854-1855.

[63] E. Chamorro, P. K. Chattaraj and P. Fuentealba, *J. Phys. Chem. A*. 2003, **107**, 7068-7072.

[64] H. Lee, W. I. Choi, M. C. Nguyen, M.-H. Cha, E. Moon and J. Ihm, *Phys. Rev. B* 2007, **76**, 195110.

[65] Q. Sun. Q. Wang, P. Jena and Y. Kawazoe, *J. Am. Chem. Soc.* 2005, **127**, 14582-14583.

Graphical Abstract

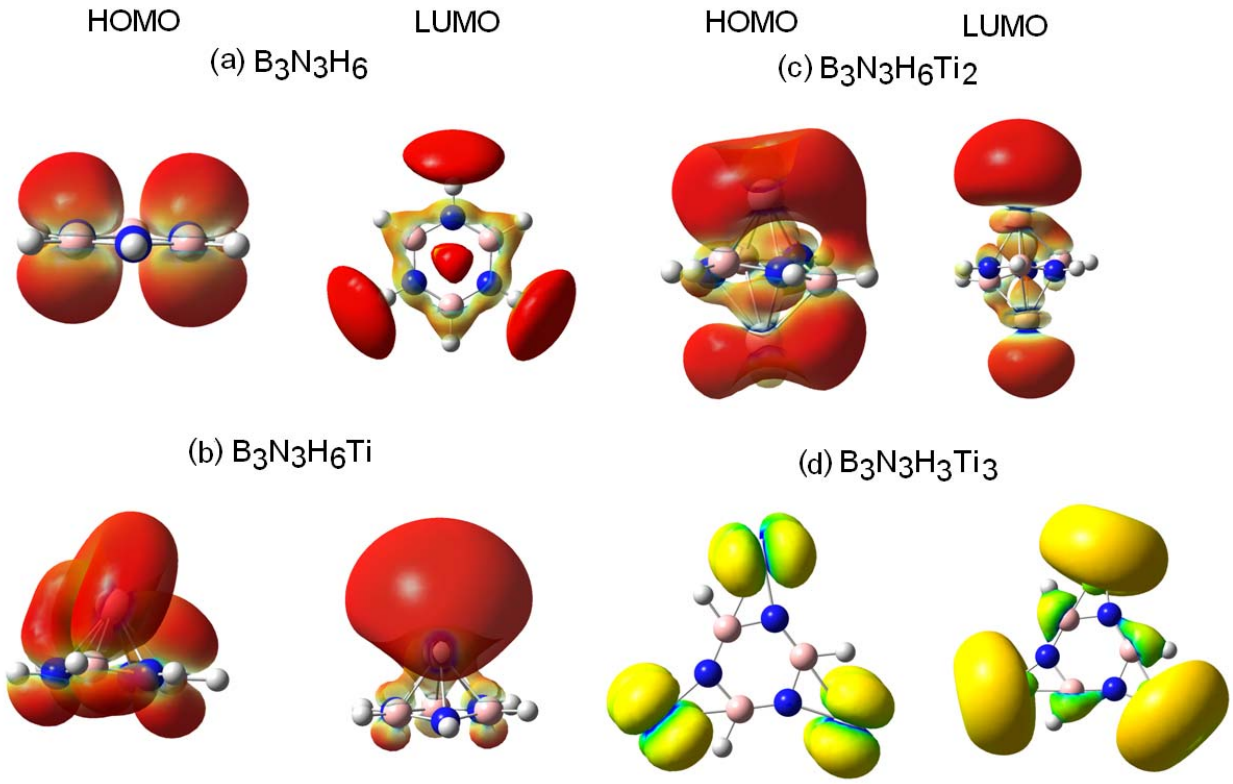

We investigate the hydrogen trapping efficiency of various metals functionalized on BN systems for potential hydrogen storage application using conceptual DFT's stability and reactivity descriptors.